Supplement Information for

Synthesis of Self-sufficient Singlet Oxygen Nanoreactor Based on Russell Mechanism with Enhanced Penetration for Cancer Therapy

Yu-e Wang[†, #], Junqiu Zhai[†, #], Yuxiu Zheng[†], Jiali Pan[†], Xiaojia Liu[†], Yan Ma[*, †], Shixia Guan[*, †]

†*School of Pharmaceutical Sciences, Guangzhou University of Chinese Medicine, Guangzhou, China.*

* Corresponding author:

Prof. Yan Ma, No. 232 Waihuan East Road, Guangzhou University of Chinese Medicine, Panyu District, Guangzhou. Phone: 86-20-39356872; Email: mayan2006@gzucm.edu.cn

Prof. Shixia Guan, No. 232 Waihuan East Road, Guangzhou University of Chinese Medicine, Panyu District, Guangzhou. Phone: 86-20-39358043; Email: drguan@gzucm.edu.cn

#Y. W. and J. Z. contributed equally to this work.

Materials

Linoleic acid, and lipoxygenase were purchased from Sigma-Aldrich. Singlet Oxygen Fluorescent Green (SOSG), Caspase inhibitor Z-VAD-FMK, Necorostatin-1, and Coumarin 6 (C 6) were obtained from Meilun Biological Co., Ltd. Calcein/PI cell viability and cytotoxicity detection kit, apoptosis and necrosis detection kit, DCFH-DA reactive oxygen species detection kit, and DAPI were bought from Shanghai Biyuntian Biotechnology Co., Ltd. Annexin V-FITC/PI double staining apoptosis detection kit was acquired from Shanghai Beibo Biotechnology Co., Ltd. Hexadecanoic acid-RRRRRRR (HA-R7), hexadecanoic acid-CRGDKGPDC (HA-iRGD), hexadecanoic acid-RRRRRRRCRGDKGPDC (HA-R7-iRGD), and hexadecanoic acid-RRRRRRNAACRGDKGPDC (HA-R7-NAA-iRGD), and Necrosulfonamide were synthesized by MedChemExpress. Amiloride, β-Cyclodextrin (β-CD), Quercetin, and Chlorpromazine were attained from Shanghai Aladdin Reagent Co., Ltd. Cell membrane dark red fluorescent probe (Dir) was gained from Shanghai Yisheng Biotechnology Co., Ltd. C11 BODIPY$^{581/591}$ was purchased from Glpbio. Recombinant Alexa Fluor® 555 fluorescent anti-calreticulin antibody (ab275117) and recombinant anti-HMGB1 antibody (ab213256) were obtained from Abcam. PerCP-Cy5.5-CD45 monoclonal antibody, BV605-CD3e monoclonal antibody, APC-Cy7-CD4 monoclonal antibody, BV650-CD8a monoclonal antibody , PE-CD25 monoclonal antibody, BV421-FoxP3 monoclonal antibody, Alexa 647-CD206 monoclonal antibody, FITC-CD11b monoclonal antibody, BV480-F4/80 monoclonal antibody, and Fixable Viability Stain 700 were bought from BD Biosciences. CD16/CD32 monoclonal antibody, PE-CD86 monoclonal antibody, APC-CD80 monoclonal antibody, and Percp-Cy5.5-CD11c monoclonal antibody were purchased from eBioscience™, Thermo Fisher Science. Mouse TNF-α ELISA kit was obtained from Shenzhen Xinbosheng Biotechnology Co., Ltd. Mouse IL-6 ELISA Kit was attained from Hangzhou Link Biotechnology Co., Ltd.

Experiment Methods

Synthesis of linoleic acid hydroperoxide. An aliquot of 0.5 g of linoleic acid

(Sigma-Aldrich, America) was mixed with 120 mL of 0.2 M sodium borate buffer (pH = 9) under magnetic stirring to emulsify the mixture. The 2 mL of lipoxidase (lipoxidase from soybean, Type I-B, Sigma-Aldrich, America) solution [6×10^4 U] was added and allowed for reaction under O_2 pressure. The temperature was kept between 0~4 °C during the whole reaction. The reaction was monitored by withdrawing an aliquot of the solution and dissolved in ethanol (10 μL/3 mL) by UV analysis, which indicated the formation of conjugated double bonds for linoleic acid hydroperoxide by an adsorption peak at 234 nm. After 4 h of reaching the maximum of adsorption at 234 nm, the solution was added with 1M of H_2SO_4 to adjust the pH to a value of 4.0. Immediately, the product was distracted by adding an excess of cold ethyl ether and washed 3 times. The ethyl ether was removed by rotary evaporation to obtain the raw product as a colorless liquid. The raw product was dissolved in ethyl acetate and then was added to column chromatography on silica gel (200 mesh). The pure LAHP was obtained through petroleum ether (30~60℃)/ ethyl acetate = 10/1~2/1gradient elution. The pure product was further analyzed by LC-MS, HNMR, and FTIR.

pH-Dependent $^1O_2$ Generation by Cu NPs. A fluorescence singlet oxygen sensor green (SOSG) and was employed to evaluate the singlet oxygen generation of linoleic acid hydroperoxides in the presence of catalytic Cu2+ ions released from Cu NPs. Briefly, 10μL of Cu NPs suspension and 10μL of SOSG (1 mM in ethanol) were added into 0.98 mL PBS (67 mM, with pH values 7.4, 6.5, 5.5, 5.0). The mixture solution was placed at an oscillating

incubator under 37°C in dark. The fluorescence of the solution was measured at 1, 4, 12, 24, and 36 h under excitation at 488 nm as the background for comparison purposes. The samples containing only Cu NPs or SOSG were used as control groups. The singlet oxygen generation of linoleic acid hydroperoxides was quantified by comparing the SOSG fluorescence enhancement with the background or control samples.

Cell culture. Cervical cancer cell line (Hela cells) was cultured in a DMEM medium supplemented with 10% (v/v) fetal bovine serum (FBS), penicillin (100 U/mL), and streptomycin (100 μg/mL) at 37°C under 5% CO2. The cells were routinely harvested by the use of trypsin and were resuspended in a fresh complete medium before plating. The culture of MCF-7, MDA-MB-231, A549, HepG2, and 4T1 cells was the same as the HeLa cells. The incubation of the pancreatic cancer cell line (Bxpc-3) and human bronchial epithelium cell line (Beas-2B) were almost the same as the HeLa cells except that the DMEM was replaced by RPMI-1640.

Living and dead cell co-staining experiment. BxPC-3 cells and Hela cells were seeded into the 12-well cell culture plate (1.5×10^4 cells per well) with 12-well round cell culture slides and cultured for 24 h. LAHP-M NPs of different concentrations were placed on wells and incubated for another 12 h. The therapy effect was detected by a fluorescence microscope (Olympus BX53, Olympus, Japan) after co-staining with calcein AM (1000X) and PI (1000x) in staining buffer solution for 30 min at 37°C. Green fluorescence of calcein AM

(Ex/Em=494/517 nm) indicated living cells and red fluorescence of PI (Ex/Em=535/617 nm) represented dead cells.

Hoechst staining and IncuCyto long-term dynamic imaging. Hoechst 33258 staining and real-time cell live imaging were used to observe the morphological changes of dead cells. Hoechst staining of macrophages involved a Hoechst staining kit (Beyotime Institute of Biotechnology). BxPC-3 cells and Hela cells treated with different concentrations of LAHP-M NPs for 24 h, were fixed and stained with Hoechst 33258(5 mg/mL) for 5 min. Cells were washed twice with PBS and were then observed under a fluorescence microscope for condensed or fragmented apoptotic nuclei. BxPC-3 cells were incubated with different concentration of LAHP-M NPs and the real-time cell live imaging of the cells were observed using the IncuCyto long-term dynamic imaging system (Essen Bioscience, IncuCyte Zoom, Germany).

Specific inhibitors rescue cell death. The cell death form was confirmed by measuring the cell viability upon coincubation with apoptotic or necrotic cell death pathway inhibitors. Z-VAD-FMK (ZVAD, 20 μM), necrostatin-1 (Nec-1, 10 μM) and Necrosulfonamide (NSA, 5μM) and Cu NPs (20 μg/mL) were added and coincubated for 12 h. The cell viability was tested by MTT assay.

Detection of Intracellular ROS in vitro

Intracellular general ROS measurement. The intracellular general ROS induced by LAHP-M NPs was determined using the DCFH-DA ROS assay kit (Beyotime Institute of Biotechnology). BxPC-3 cells or Hela cells were seeded

into a 12-well cell culture plate (1.5×10^5 cells per well, within cell culture slides) and cultured for 24 h. Different concentrations of LAHP-M NPs were added into the well for 4 h of co-incubation. Afterward, the cells were washed, co-incubated with DCFH-DA testing fluid (10 μM) for an additional 30 min, fixed, and stained with Hoechst for observation on the fluorescence microscope (Olympus BX53, Olympus, Japan).

Detection of intracellular lipid peroxides. Intracellular lipid peroxides were detected via BODIPY$^{581/591}$ C11 (GLPbio, America) following manufacturers' instructions. Hela cells were seeded in 24-well plates at a density of 1×10^5 cells per well and incubated overnight. The medium was replaced with a different concentration of Cu NPs for a 4 h incubation. Then, the BODIPY$^{581/591}$ medium (2.5 μM in PBS) was added to the cells and incubated for 30 min in dark. Fixed the cells and stained with Hoechst to observe on the fluorescence microscope (Olympus BX53, Olympus, Japan).

3D tumor spheroids growth inhibition assay. 3D Hela spheroids were treated with different concentrations of polypeptide-modified LAHP-M NPs for 3 days. The integrity and diameter of the spheroids were monitored with an IncuCyto long-term dynamic imaging system (Essen Bioscience, IncuCyte Zoom, Germany) evryday. At the endpoint, the tumor spheroids viability was tested using a Living/Dead cell co-staining Kit (Beyotime Institute of Biotechnology). The tumor spheroids were incubated with calcein AM (1000X) and PI (1000x) for 30 min and images of the spheroids were taken with IncuCyto long-term dynamic imaging system. The images were analyzed by Image-Pro Plus 6.0 (Media Cybernetics, Inc., America) and the

ratio of green fluorescence and red fluorescence was indicating the viability of the tumor spheroids.

***In vivo* biodistribution.** Hela-bearing nude mice were randomly divided into three groups with six mice in each group. PBS, Cu NPs, and Cu-NAA NPs (10 mg/kg) were tail-intravenous (i.v.) injected into each group. 24 h later, the mice were sacrificed and the major organs (including the heart, liver, spleen, lung, kidney) were separated, weighed, and ground. The ground organ was digested using HNO_3 for 2 days, and following this, diluted to a 5% HNO_3 solution in water. The Cu content was determined with an ICP-MS apparatus and the results were compared with the Cu references. The tissue retention rate of copper was calculated according to the following formula.

$$Tissue\ retention\ rate\left(\%\frac{ID}{g}\right) = \frac{\frac{Cu\ content\ of\ NPs\ grous}{tissue\ weight} - \frac{Cu\ content\ of\ PBS\ grous}{tissue\ weight}}{total\ injected\ Cu\ content} \times 100\%$$

***In vivo* $^1O_2$ measurement.** The SOSG probe was used to detect the generation of $^1O_2$ in tumor tissues after continuous administration. One day after the end of the last administration, the nude mice of the PBS group and Cu-NAA NPs were injected intratumorally with the singlet oxygen probe SOSG (50 μM). The nude mice were sacrificed 24 hours later and the tumor was separated. The tumor was quick-frozen and cut into 7 μm thick tissue slices. The slices were stained with DAPI and observed on the fluorescence microscope (Olympus BX53, Olympus, Japan).

CRT and HMGB1 detection. To study the ROS-mediated cancer therapy effect on tumor immune, the damage-associated molecular patterns (DAMPs) signals including CRT and HMGB1 were detected. In detail, for CRT detection, Hela cells on cell culture slides were incubated with PBS and Cu-NAA NPs (20 μg/mL) for 12 h. Subsequently, the cells were stained by Alexa Fluor 555 conjugated anti-CRT monoantibody (ab275117, 1/100 dilution, Abcam) for 30 min and rinsed with PBS three times. As for HMGB1 detection, Hela cells were assigned to PBS and Cu-NAA NPs (20 μg/mL) for 12 h and then were fixed and permeabilized with 0.1% Triton X-100 in PBS for 10 min. Subsequently, the cells were blocked with 2% FBS and stained by anti-HMGB1 monoantibody (ab213256, 1 μg/mL, Abcam) overnight. Then, 1 μM FITC-anti-IgG (second antibody) was used to label the HMGB1 in the nucleus of Hela cells. The cell nuclei were stained by DAPI. At last, the images of the cells were obtained by a fluorescence microscope (Olympus BX53, Olympus, Japan).

***In vitro* dendritic cells maturation analysis.** To verify that DAMPs released from dead cells enable dendritic cells to mature, the experiment was conducted through a dendritic cell-dead cells co-incubation model. In brief, Hela cells or 4T1 cells were seeded in the upper chamber of a 12-well Transwell plate at 5×10^4 cells/chamber, and DC2.4 cells were seeded in the lower chamber at 10×10^4 cells/chamber. After co-incubation for 24 h, the cells in the upper chamber were administrated with PBS and Cu-NAA NPs (20 μg/mL) for 6 h, then replaced with fresh medium. 24 h later, DC2.4 cells in the lower chamber

were collected, blocked with CD16/32 (1 μg/per tube) and stained with anti-CD11c-PerCP/Cyanine5.5, anti-CD80-PE, and anti-CD86-APC (Invitrogen) for 30 min at 4°C, and then evaluated by flow cytometry (ACEA NovoCyte Quanteon Flow Cytometry, Agilent, America).

Supplemental figures and tables

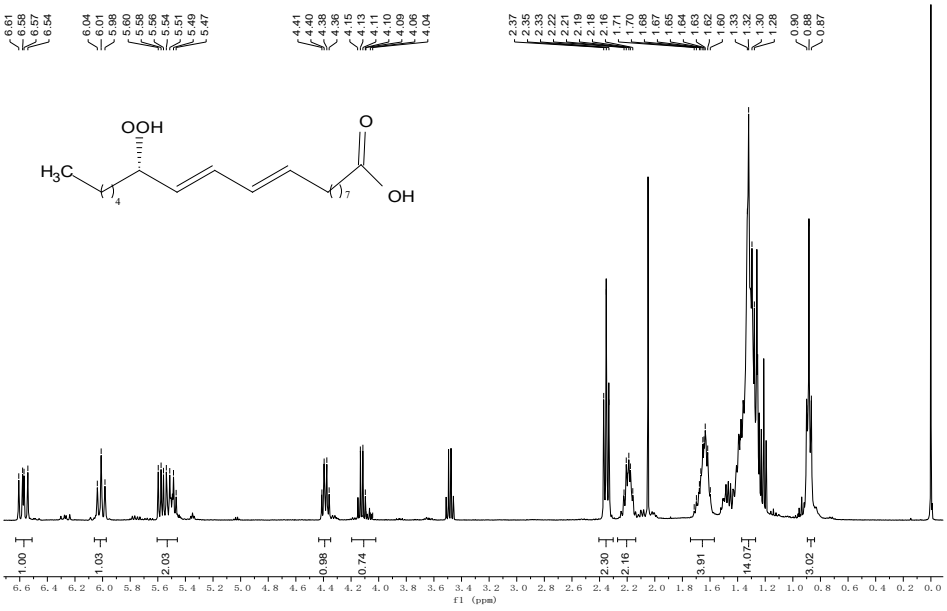

Figure S1 The H-NMR spectrum of LAHP

^{1}H NMR (400 MHz, Chloroform-*d*) δ 6.63 – 6.53 (m, 1H), 6.08 – 5.94 (m, 1H), 5.61 – 5.43 (m, 2H), 4.39 (dt, *J* = 8.2, 6.6 Hz, 1H), 4.12 (q, *J* = 7.2 Hz, 1H), 2.35 (t, *J* = 7.4 Hz, 2H), 2.19 (dddt, *J* = 8.7, 7.1, 3.9, 1.6 Hz, 2H), 1.65 (ddt, *J* = 14.8, 12.2, 7.2 Hz, 4H), 1.40 – 1.25 (m, 14H), 0.95 – 0.81 (m, 4H).

Table S1 Particle size, PDI and Zeta potential of polypeptide-modified LAHP-M NPs (n=3， $\bar{x}\pm S$)

samples	Size（nm）	PDI	Zeta pontential (mV)
Cu NPs	155.38±5.068	0.169±0.022	-25.70±0.777
Cu R7 NPs	136.60±2.051	0.112±0.028	15.20±1.76
Cu iRGD NPs	150.90±3.253	0.038±0.035	-12.50±0.252

Cu R7-iRGD NPs	86.68±2.128	0.072±0.001	16.70±1.59
Cu-NAA NPs	136.10±5.515	0.086±0.043	17.70±0.751
Fe NPs	120.33±2.881	0.122±0.008	-19.43±0.757
Fe R7 NPs	104.5±1.414	0.169±0.025	38.40±0.721
Fe iRGD NPs	97.14±2.072	0.137±0.028	-0.127±0.299
Fe R7-iRGD NPs	97.44±2.284	0.207±0.003	34.40±1.10
Fe-NAA NPs	115.30±0.07	0.150±0.025	37.80±0.451

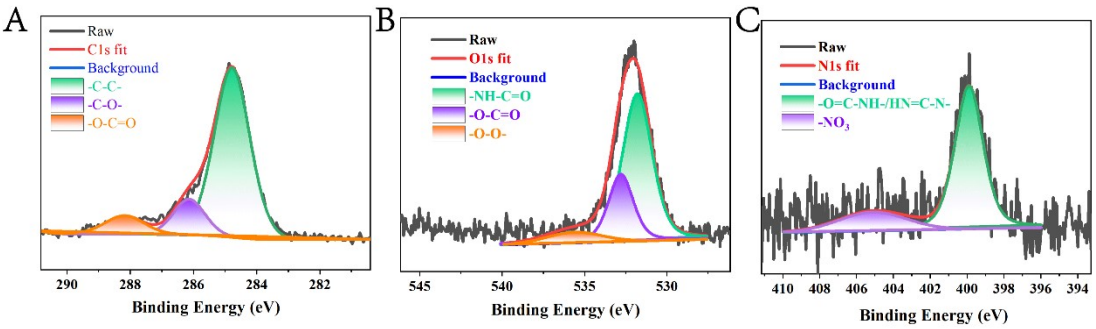

Figure S2 High-resolution C1s (K), O 1s (L), N1s (M), S1s(N)of Cu-NAA NPs.

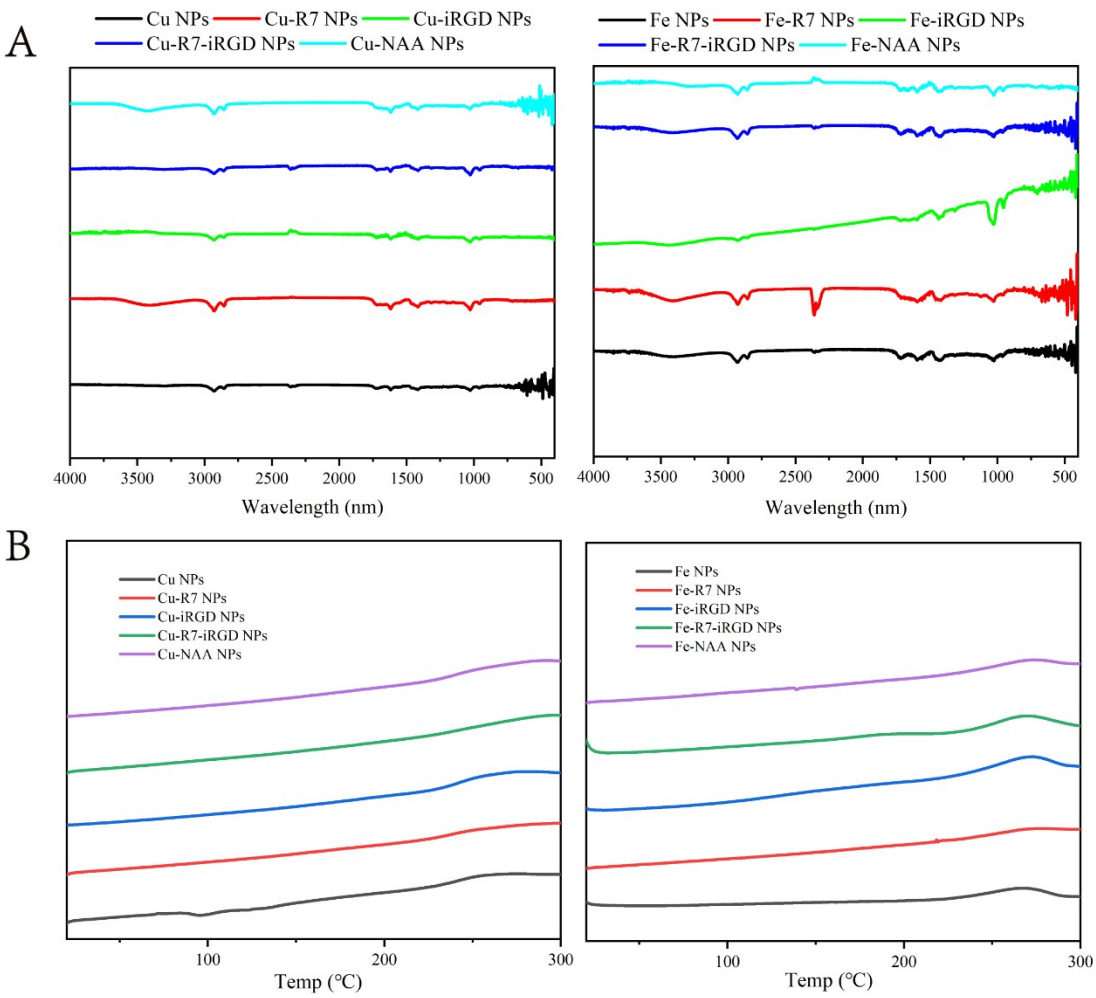

Figure S3 FTIR spectra (A) and DSC curves (B) of LAHP-M NPs and polypeptide-modified LAHP-M NPs.

Table S2 Comparison of IC50 of LAHP-M NPs on different cell lines (μg/mL, n=3)

Cell lines	Cu NPs	Fe NPs
MCF-7	13.210 ± 0.354	21.646 ± 0.561
MDA-MB-231	20.210 ± 0.235	12.210 ± 0.652
Hela	14.540 ± 0.157	14.654 ± 0.205
A549	15.935 ± 0.478	17.867 ± 0.685
HepG2	9.426 ± 0.546	13.099 ± 0.856
BxPC-3	14.548 ± 0.253	12.133 ± 0.351

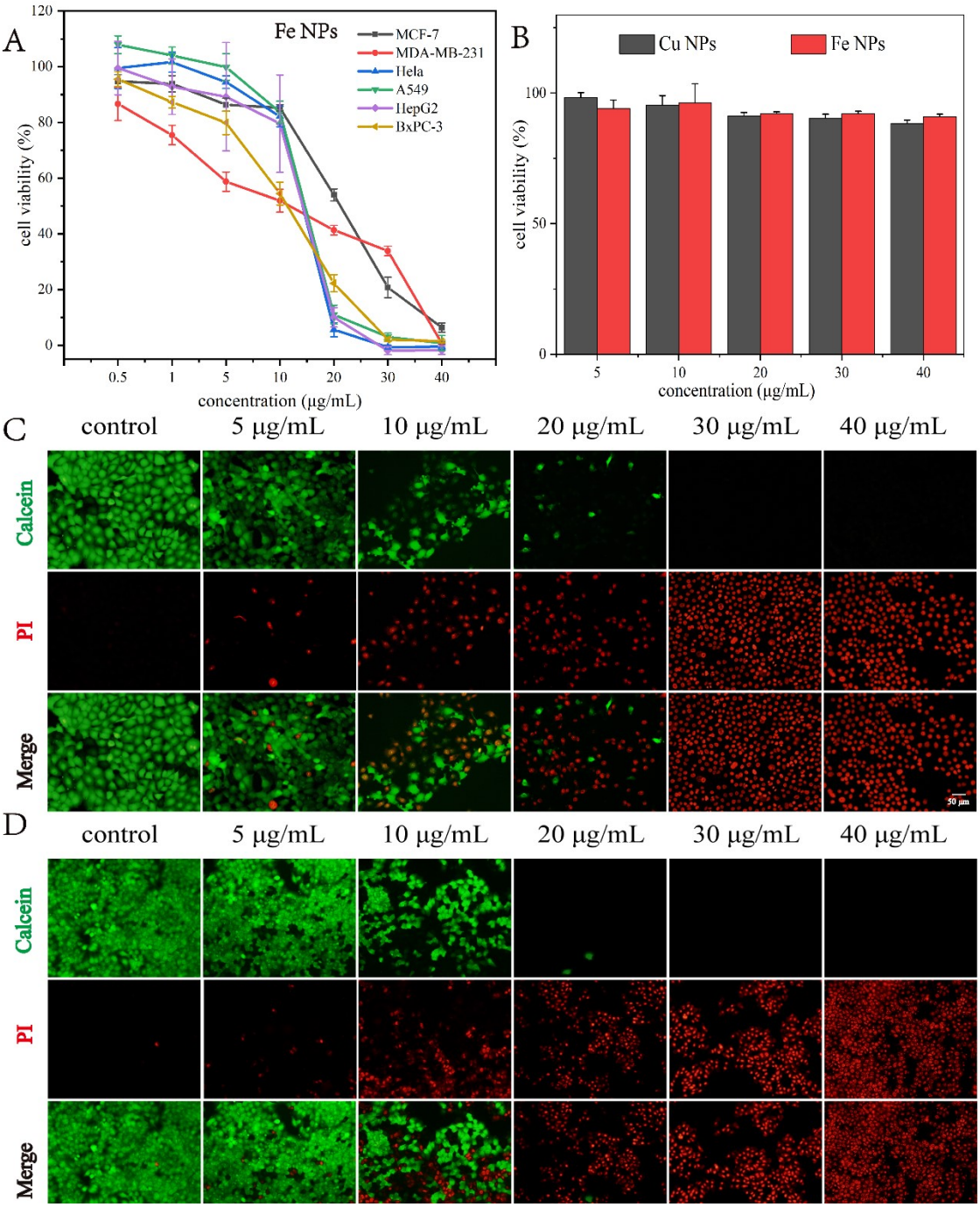

Figure S4 *In vitro* cytotoxicity in 2D cultured cells. (A) *In vitro* cytotoxicity of Fe NPs towards MCF-7, MDA-MB-231, Hela, A549, HepG2, and BxPC-3 cells upon 24 h treatment with different concentrations. (B) *In vitro* cytotoxicity of LAHP-M NPs towards normal cells (Beas-2B cells). Live(green)/dead(red) staining BxPC-3 cells (C) and Hela cells (D) administrated with different concentrations of Fe NPs for 24 h were observed using fluorescence microscopy (scale bar, 50 μm).

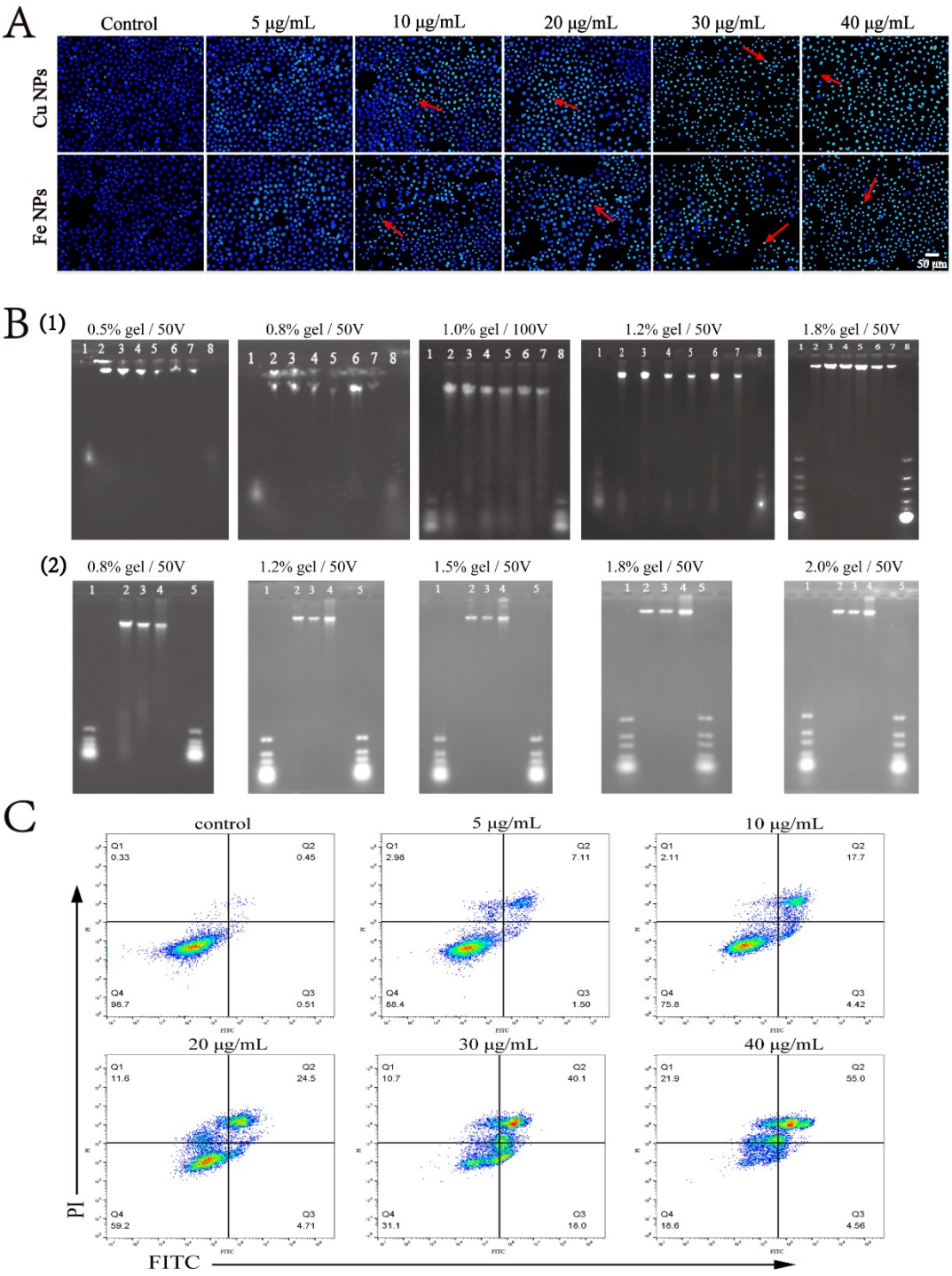

Figure S5 The form of cell death. (A), fluorescent micrographs of BxPC-3 cells stained by Hoechst33258 after incubation with different concentrations of LAHP-M NPs for 24 h (scale bar, 50 μm). (B), for (1), 1, 8 repesent DNA markers; 2, 3 are from control groups, 4, 5 are from Cu NPs group; 6, 7 are from Cu-NAA NPs group; for (1) 15 μg/mL Cu NPs were incubated for 0 h (labeled as 2), 6 h (labeled as 3), and 12 h (labeled as 4) after administration, 1 and 5 represent DNA markers. (C),

Representative Annexin V-FITC & PI flow cytometry plot for HeLa cells incubated with different concentrations of Fe NPs for 24 h. Q1 (left top): necrotic cells, Q2 (right top): late apoptotic/necrotic cells, Q3 (right bottom): early apoptotic cells, and Q4 (left bottom): viable cells.

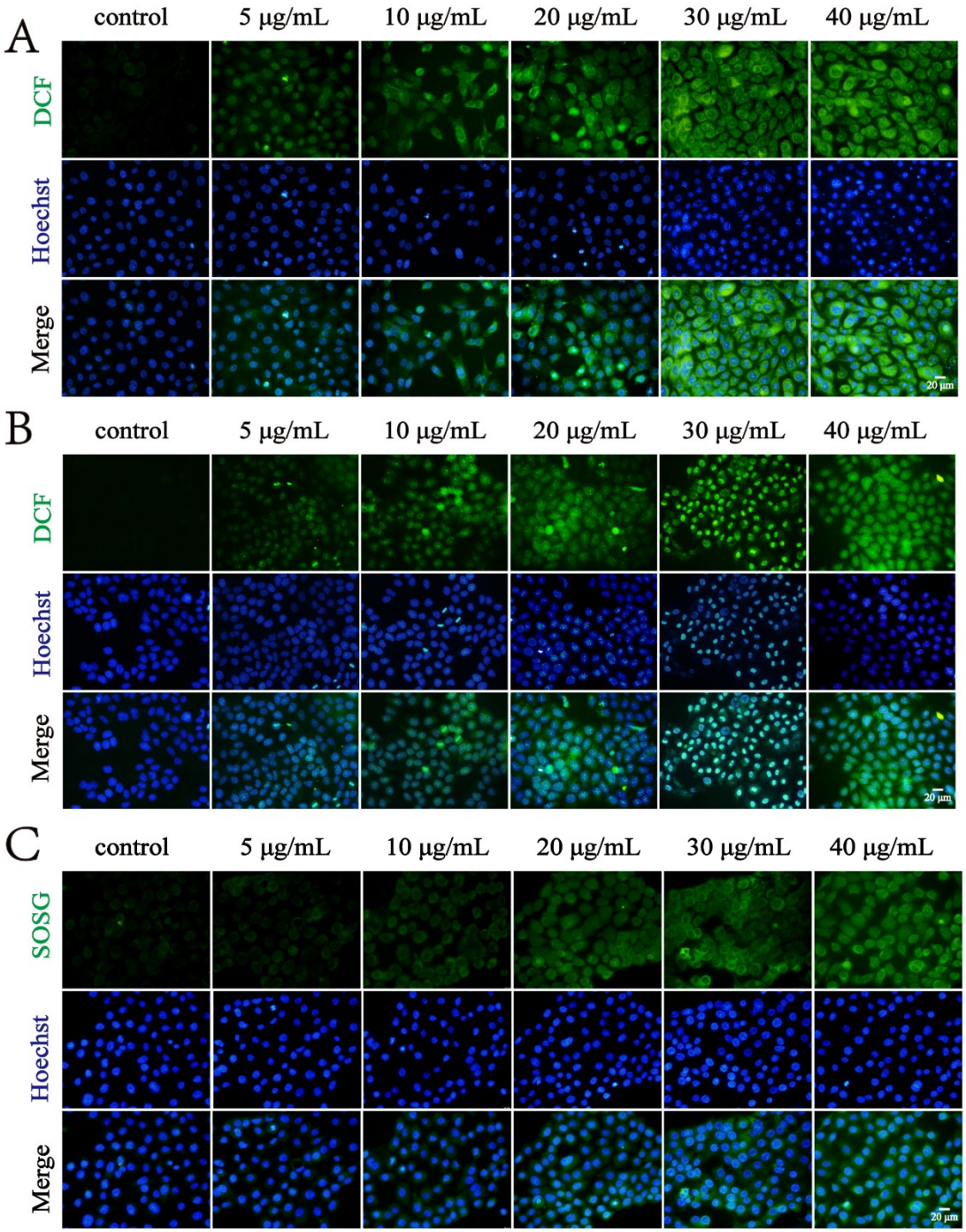

Figure S6 Intracellular ROS generation *in vitro*. General ROS generation was measured by DCFHDA (green) prob in BxPC-3 cells (A) and Hela cells (B) induced

by Fe NPs. Activatable $^1O_2$ generation detected by SOSG (green) from Fe NPs in Hela cells (C).

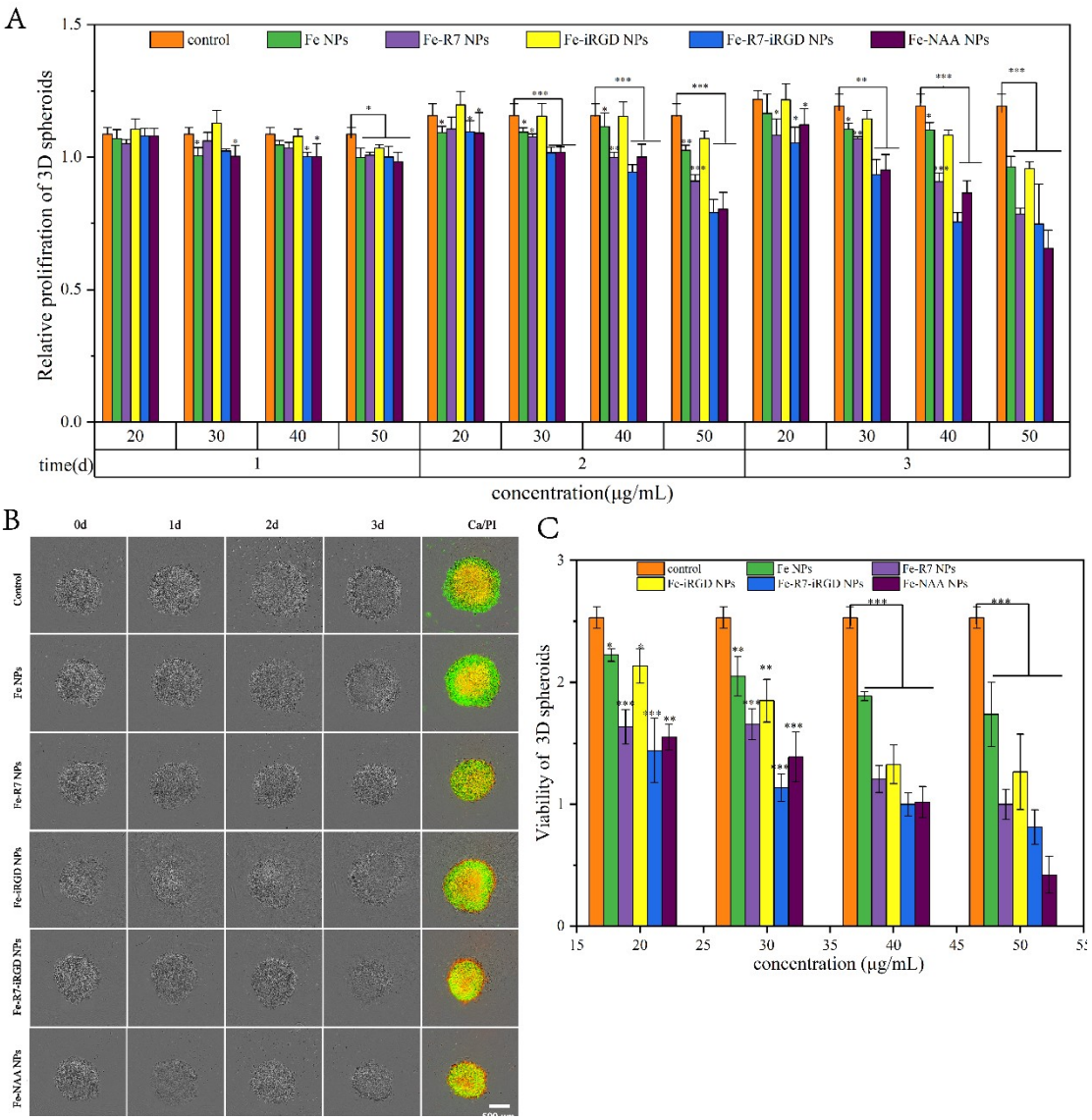

Figure S7 ***In vitro*** **anticancer efficacy against 3D tumor spheroids.** Relative proliferation of 3D spheroids (A) upon polypeptide-modified Fe NPs treatment for three days. (B), representative graphs of 3D tumor spheroids administrated by 40 μg/mL polypeptide-modified Fe NPs on days 0, 1, 2, 3, and the spheroids were stained by Calcein AM/PI on day 3. (C), relative cell viability of 3D spheroids assayed by the ratio of green(live)/red(dead) fluorescence on day 3. All the statistical *p* values were calculated by the one-way *ANOVA* with the *Bonferroni* multiple comparison test (mean ± sd. $n = 3$). *$p < 0.05$, **$p < 0.01$, ***$p < 0.001$, compared with the control group.

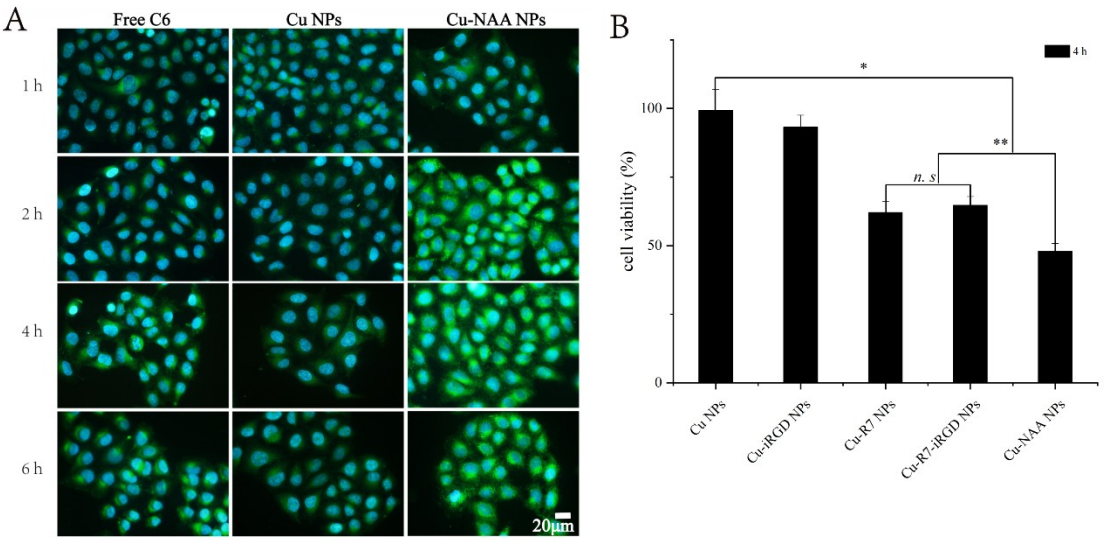

Figure S8 Intracellular delivery against Hela cells. (A), uptake of Dir labeled polypeptide modified- and nude- Cu NPs in Hela cells. Cells were incubated with Dir labeled polypeptide modified- and nude- Cu NPs (10 μg/mL) for different times and were stained with Hoechst 33258 for nucleus directive. Images were acquired at 15 min, 0.5, 1, 2, 4, 6 h by a fluorescence microscope (Scale bar = 20 μm). (B), cell viability measured by MTT test against Hela cells after incubation with polypeptide modified- and nude- Cu NPs for 4 h. The cytotoxicity of polypeptide modified- and nude- Cu NPs coincided with the cellular uptake of the NPs, indicating that polypeptide modification enhanced the cellular internalization of nude- Cu NPs. All the statistical p values were calculated by the one-way *ANOVA* with the *Dunntt'T3* multiple comparison test (mean ± sd. $n = 6$). n.s, no significance, *$p < 0.05$, **$p < 0.01$.

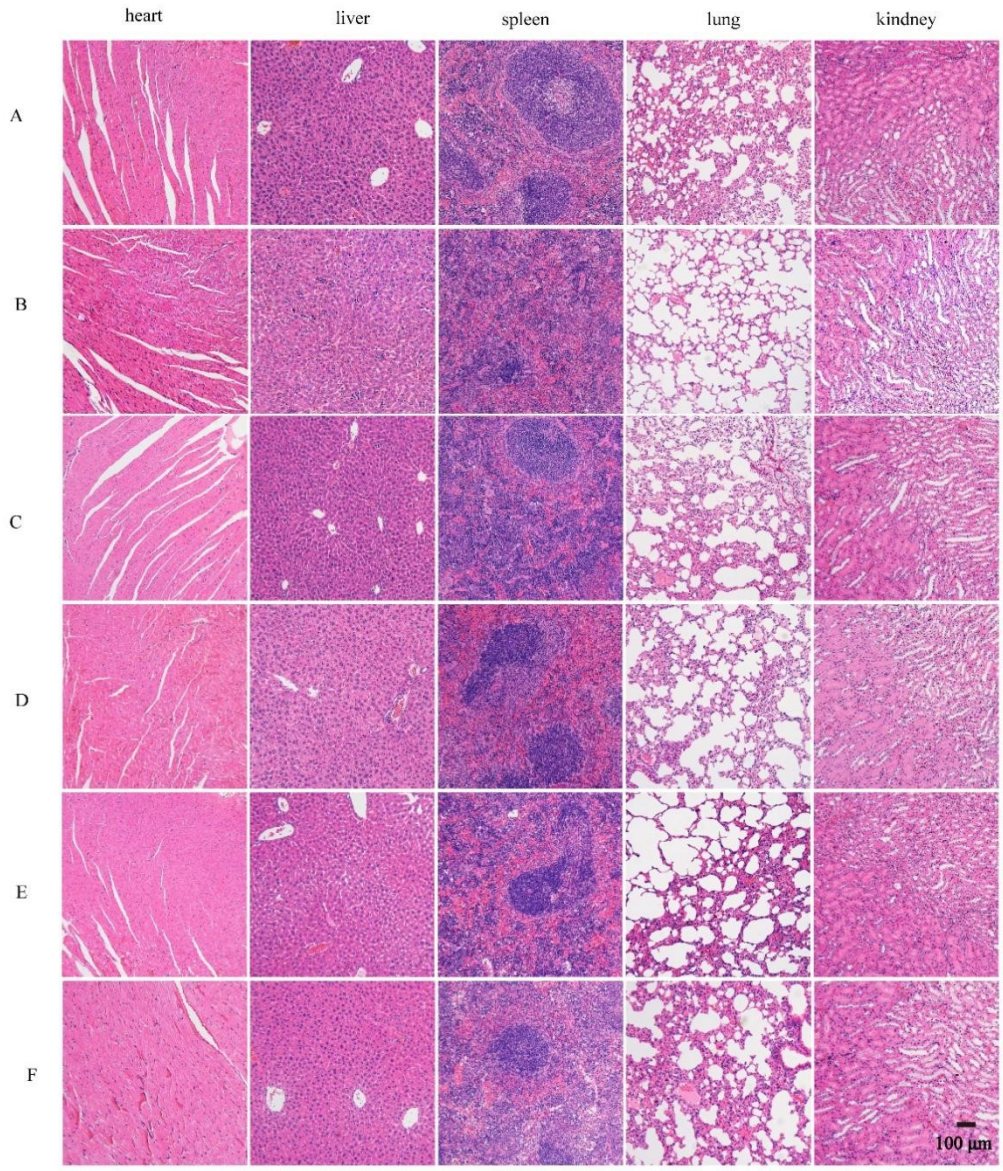

Figure S9 Representative H&E stained images of major organs from treated mice. (A), control. (B), Cu NPs. (C), Cu-R7 NPs. (D), Cu-iRGD NPs. (E) Cu-R7-iRGD NPs. (F), Cu-NAA NPs. (Scale bar: 100 μm)

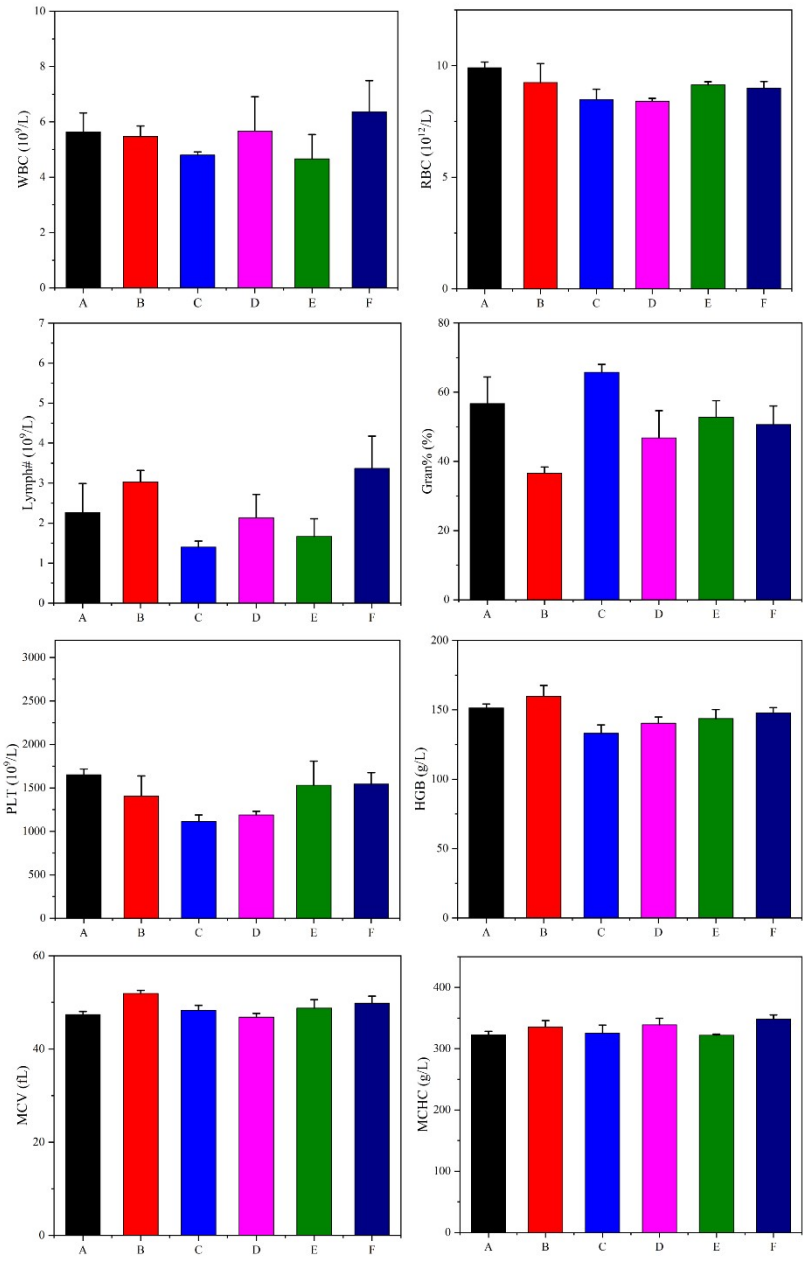

Figure S10 Blood test includes WBC, RBC, Lymph#, Gran%, PLT, HGB, MCV, and MCHC in different treatment groups. (A), control. (B), Cu NPs. (C), Cu-R7 NPs. (D), Cu-iRGD NPs. (E) Cu-R7-iRGD NPs. (F), Cu-NAA NPs.

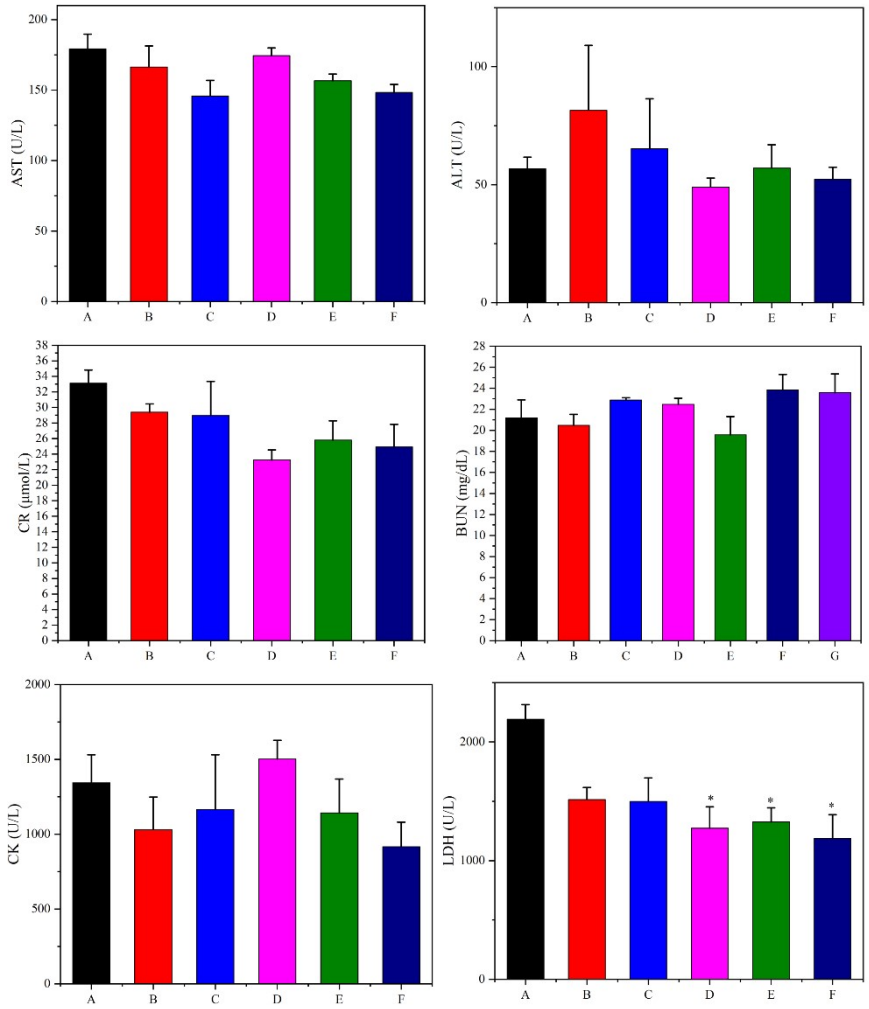

Figure S11 Blood biochemistry analysis includes ALT, AST, CR, BUN, CK and LDH in different treatment groups. (A), control. (B), Cu NPs. (C), Cu-R7 NPs. (D), Cu-iRGD NPs. (E) Cu-R7-iRGD NPs. (F), Cu-NAA NPs. The statistical *p* values were calculated by the one-way *ANOVA* with *Bonferroni* or *Dunntt'T3* multiple comparison test (mean ± sd. $n = 3$). *$p < 0.05$.

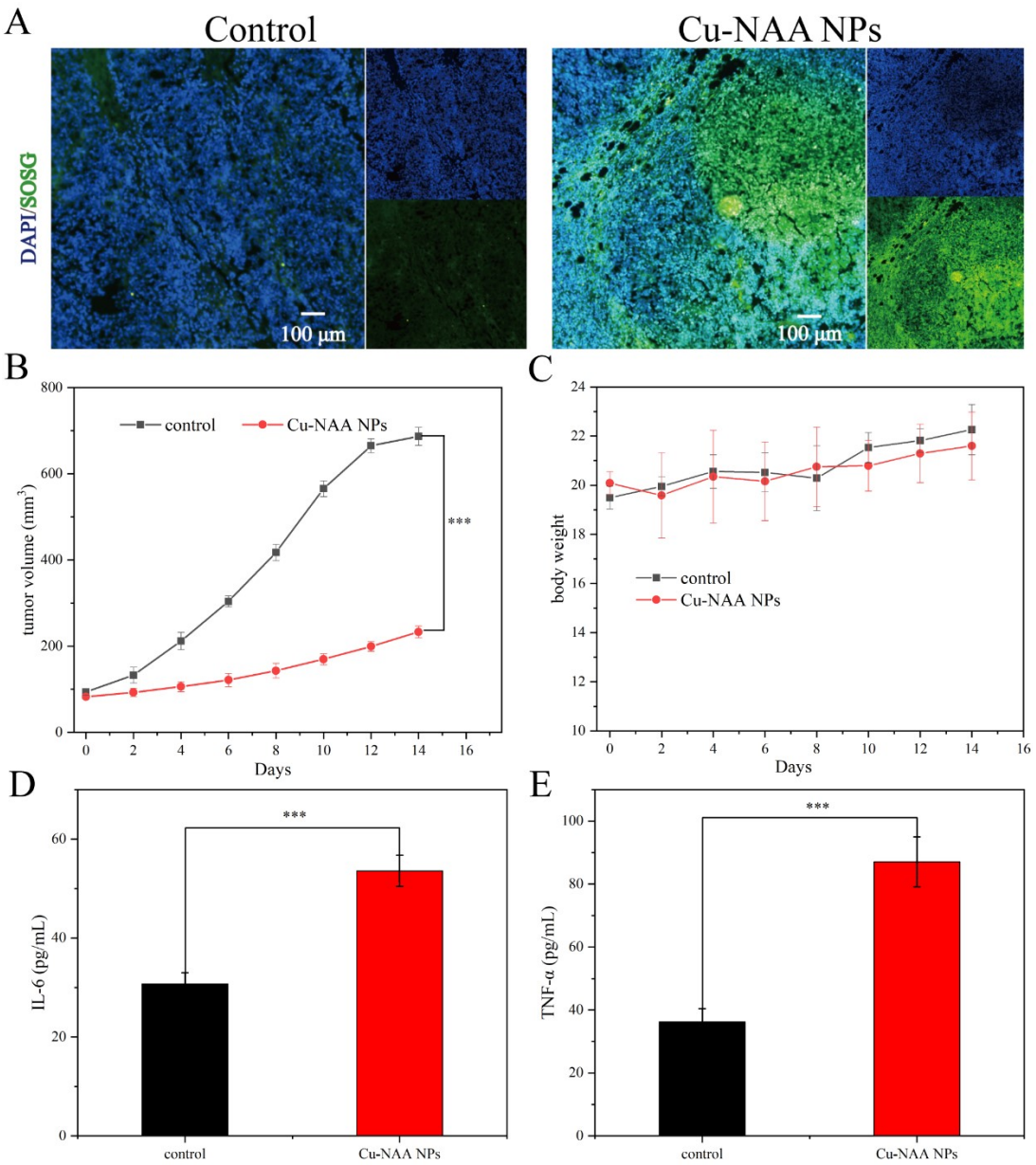

Figure S12 *in vivo* $^1O_2$ generation and immune response in 4T1 tumor-bearing mice. (A) *in vivo* $^1O_2$ generation measured by SOSG after continuous dosing of PBS and Cu-NAA NPs. Tumor volume (B) and body weight (C) change curves after different in 4T1 tumor-bearing mice model. IL-6 (D) and TNF-α (E) content in blood serum samples. All the statistical *p* values were calculated by the two samples *t* test (mean ± sd. $n = 3$). ***$p < 0.001$.